Chiral 1D Cyanide-Bridged Bimetallic Compounds Build With Enantiomorphic Pentagonal Bipyrimidal M(II) Units

Dylan Martinez, Céline Pichon, Carine Duhayon, Virginie Béreau, Hironori Yamaguchi, Jean-pascal Sutter

EurJIC
European Journal of Inorganic Chemistry

Research Article
doi.org/10.1002/ejic.202400449

Chemistry Europe
European Chemical Societies Publishing

www.eurjic.org

Chiral 1D Cyanide-Bridged Bimetallic Compounds Build With Enantiomorphic Pentagonal Bipyrimidal M(II) Units

Dylan Martinez,[a] Céline Pichon,[a] Carine Duhayon,[a] Virginie Béreau,[a, b] Hironori Yamaguchi,[c, d] and Jean-Pascal Sutter*[a]

Chiral 1D coordination compounds formed by association of either of the enantiomers of [ML(MeOH)Cl]Cl (with M=Mn^{II} or Fe^{II}; L stands for either *R* or *S* enantiomer of a pentadentate macrocycle) and $NBu_4[Fe^{III}(bpb)(CN)_2]$, namely: 1D-[{$Fe^{III}$-(bpb)$(CN)_2$}{$M^{II}(L^R)$}]$(PF_6)$ and 1D-[{Fe^{III}(bpb)$(CN)_2$}{$M^{II}(L^S)$}](PF_6) with M=Mn (**2R**, **2S**) and Fe (**3R**, **3S**). The bis(triphenylphosphine)iminium salt of the metallo-ligand, $PNP[Fe^{III}(bpb)(CN)_2]\cdot 2H_2O$, **1 b**, is also described. Their preparations, crystal structures, optical and magnetic properties are reported. Mössbauer spectroscopy confirmed the oxidation state in the [Fe^{II}–Fe^{III}] chain, for which AC susceptibility suggests SCM behavior, but for very low *T*.

1. Introduction

Molecular magnetic compounds have been a subject of extensive research since several decades. Designs and specific chemical approaches have been explored in order to access specific materials with controlled properties.[1–10] The latest developments are aimed at materials in which magnetic properties combine with other properties, ideally in a synergistic way.[11–14] In many cases, this crossover of properties is induced by asymmetry, as in the case of multiferroics or for magneto-optic effects. Chirality control is therefore an additional parameter to be taken into account when designing these materials.

Single-chain magnets (SCMs) belong to the magnetic compounds of current interest. These molecular nanomagnets are exchange-coupled 1D spin arrays characterized by a freezing of their magnetization below a threshold temperature.[15,16] Such a behavior results from an easy-axis magnetic anisotropy for the chain which is induced by individual magnetic centers exhibiting themselves axial anisotropy, i.e. a negative axial zero field splitting (ZFS) parameter *D*. In this respect, metal complexes with pentagonal bipyramidal (PBP) geometry have proven to be well-suited building blocks, especially Fe^{II} and Ni^{II} derivatives for which *D* is typical between −10 and −20 cm^{-1}.[17] Such complexes have been successfully involved in the preparation of SCMs.[18–22] Herein, we explored the possibility of achieving chiral cyano-bridged 1D coordination polymers involving PBP centers stabilized by a pentadentate macrocycle.

Chiral 1D coordination polymers are classically built from metal complexes bearing homochiral ligands.[23–29] Recently, we have reported the preparation of a chiral PBP Fe^{II} derivative based on an homochiral macrocyclic ligand (L^R and L^S, Scheme 1).[30] Its exchangeable apical coordination sites and magnetic anisotropy make it an interesting precursor for the development of chiral chains. The possibility of forming 1-D coordination polymers by association with a *trans*-dicyanido metallo-ligand was therefore investigated. The metallo-ligand $[Fe^{III}(bpb)(CN)_2]^-$ (bpb^{2-} stands for 1,2-bis(pyridine-2-carboxamido)benzenate(2−), Scheme 1) was chosen as the assembling unit due to the *trans* position of the cyanido groups, which favors a linear arrangement of a 1D polymer.[21,31,32] This metallo-ligand was reported to lead to hetero-metallic cyanido-bridged compounds with Mn^{II},[31] Ni^{II},[32] and Cu^{II} complexes[33,34] bearing polydentate ligands in their equatorial positions. Discrete and 1D systems were obtained, but this seems to depend on the M^{II} complex rather than being controlled by the

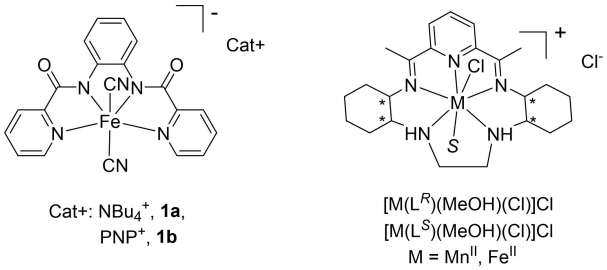

Scheme 1. Molecular units involved in the formation of the 1D coordination compounds.

[a] *D. Martinez, C. Pichon, C. Duhayon, V. Béreau, J.-P. Sutter*
Laboratoire de Chimie de Coordination du CNRS (LCC), Université de Toulouse, CNRS, 205 route de Narbonne, F-31077 Toulouse, France
E-mail: jean-pascal.sutter@lcc-toulouse.fr

[b] *V. Béreau*
Université de Toulouse, Institut Universitaire de Technologie Paul Sabatier-Département de Chimie, Av. Georges Pompidou, F-81104 Castres, France

[c] *H. Yamaguchi*
Department of Physical science, Osaka Metropolitan University, 1-1 Gakuen-cho, Naka-ku, Sakai, Osaka 599-8531, Japan

[d] *H. Yamaguchi*
Innovative Quantum Material Center (IQMC), Osaka Metropolitan University, 1-1 Gakuen-cho, Naka-ku, Sakai, Osaka 599-8531, Japan

Supporting information for this article is available on the WWW under https://doi.org/10.1002/ejic.202400449

Research Article
doi.org/10.1002/ejic.202400449

reaction conditions; a fairly common occurrence in metallo-supramolecular chemistry.[26] Interestingly, with PBP Mn^{II} derivatives, only 1D polymers were formed.[31] In addition, its paramagnetic nature, with a spin $S=\frac{1}{2}$, gave rise to exchange interactions with the metal ions bound to the CN units.

Using $[Fe^{III}(bpb)(CN)_2]^-$ as the assembling unit, 1D coordination compounds formed with either of the enantiomers of the chiral PBP Fe(II) complex, and the Mn(II) homologues, have been obtained, namely : 1D-$[\{Fe^{III}(bpb)(CN)_2\}\{M^{II}(L^R)\}](PF_6)$ and 1D-$[\{Fe^{III}(bpb)(CN)_2\}\{M^{II}(L^S)\}](PF_6)$ with M=Mn (**2R**, **2S**) and Fe (**3R**, **3S**). Their preparations, crystal structures, optical and magnetic properties are reported.

2. Results and Discussion

Syntheses. The tetrabutylammonium salt, $NBu_4[Fe^{III}(bpb)(CN)_2]$ **1 a**,[35] appeared especially suited to the assembling reaction with the chiral [ML(MeOH)Cl]Cl complexes, because of its solubility in organic solvents. The bis(triphenylphosphine)iminium salt, $PNP[Fe^{III}(bpb)(CN)_2]\cdot 2H_2O$, **1 b**, was prepared with the aim of separating the paramagnetic centers in the crystal lattice. It was used as a reference compound for the magnetic behavior of the Fe^{III} complex. Its crystal structure is also reported.

The reaction by slow inter-diffusion of MeOH solutions of $NBu_4[Fe^{III}(bpb)(CN)_2]$ and one of the enantiomer of [MnL(MeOH)Cl]Cl[36] or [FeL(MeOH)Cl]Cl[30] (with L either L^R or L^S, Scheme 1) in the presence of PF_6^- anions afforded crystalline solids of respectively, 1D-$[\{Fe^{III}(bpb)(CN)_2\}\{Mn^{II}(L)\}](PF_6)\cdot MeOH\cdot H_2O$ (**2R**, **2S** for respectively, L^R or L^S enantiomer) and 1D-$[\{Fe^{III}(bpb)(CN)_2\}\{Fe^{II}(L)\}](PF_6)\cdot H_2O$ (**3R**, **3S** for L^R or L^S enantiomer respectively). Powder X-ray diffraction studies indicated that all compounds are isostructural (see Figure S11 for diffraction patterns). The structure for **2R** was established from single-crystal diffraction studies, but the crystals of Fe derivatives **3R**/**S** were consistently too small to allow the crystal structure to be established. When ClO_4^- was used in place of PF_6^-, the crystallization process yielded crystals of $[\{Fe^{III}(bpb)(CN)_2\}\{Fe^{II}(L^R)\}](ClO_4)_{0.4}Cl_{0.6}\cdot 0.25MeOH\ 1.6H_2O$, **4R**, suitable for crystallographic studies that provided access to metrics for the Fe^{II}—Fe^{III} chain. As access to the chain structure was the sole purpose of **4R**, no further characterization was undertaken for this compound. It should be noted that all experiments and sample preparation involving the Fe^{II} derivatives were carried out in a glovebox under an Ar atmosphere, experimental details and various characterization data are given in the SI.

Crystal structures. The crystal structures for $PNP[Fe^{III}(bpb)(CN)_2]\cdot 2H_2O$, **1 b**, for $[\{Fe^{III}(bpb)(CN)_2\}\{Mn^{II}(L^R)\}](PF_6)\cdot MeOH\cdot H_2O$, **2R**, and for the perchlorate salt of the related derivative $[\{Fe^{III}(bpb)(CN)_2\}\{Fe^{II}(L^R)\}](ClO_4)_{0.4}Cl_{0.6}\cdot 0.25MeOH\ 1.6H_2O$, **4R**, have been investigated by single crystal X-ray diffraction studies. Crystal data, ORTEP plots of the asymmetric units, and metric data can be found in the Supporting Information section.

$PNP[Fe^{III}(bpb)(CN)_2]\cdot 2H_2O$, **1 b**, crystallized in the space group *P*-1. It consists in one hexacoordinated Fe^{III} complex, one PNP^+ and two H_2O solvate molecules (Figure 1). The molecular complex displays the tetradentate bpb^{2-} ligand in the equatorial coordination sites of the Fe and two C-linked CN ligands in the apical positions. The coordination sphere has a distorted octahedral shape, as shown by the shape parameter of 1.685 *versus* O_h geometry[37] deduced from Continuous Shape Measures analysis (Tables S5–S7) performed with SHAPE software.[38] Separated evaluations of axial alignment and equatorial square planar symmetry have shown that the overall distortion come from plane distortion (shape parameter: 1.689 *versus* D_{4h}) rather than axial distortion (shape parameter: 0.279 *versus* linear). Fe–C axial distances (1.971(1)–1.972(1) Å), Fe–N equatorial distances for amide moieties (1.886(1)–1.897(1) Å) and Fe–N equatorial distances for pyridine moieties (2.001(1)–2.006(1) Å) all confirm the equatorial distortion of the complex. The shortest intermolecular Fe···Fe distance is about 6.4 Å, with π-stacking between the pyridine moieties (around 3.7 Å away from each other). The pertinent bond distances and angles are given in the Figures S12 and S13; they conform that reported for other salts.[35,39]

$[\{Fe^{III}(bpb)(CN)_2\}\{Mn^{II}(L^R)\}](PF_6)\cdot MeOH\cdot H_2O$, **2R**, crystallized in the chiral space group $P2_12_12_1$. It consists in a cationic 1D coordination polymer made of Fe^{III} and Mn^{II} units, PF_6^- anions, and H_2O and MeOH solvates molecules (Figure 2). Two crystallographically distinct chain units are found in the asymmetric unit, but either consist of alternating Fe^{III} and Mn^{II} centers bridged by CN-linkers. Each $\{Fe^{III}(bpb)(CN)_2\}$ unit is linked to two Mn units by the means of the N-atoms of its cyanido-ligands and each Mn unit is connected to two Fe^{III} units through the apical sites. This results in a rather straight homochiral 1D arrangement (Figure S14). All the Mn(II) moieties display a PBP coordination sphere with the macrocyclic ligand in the equatorial coordination sites. The stereochemistry of the four asymmetric C centers of the ligand is *R*, in agreement with the stereoisomer involved in the assembling process, i.e. $[Mn L^R(MeOH)Cl]Cl$. The CShM parameters (0.380–0.378 *versus* D_{5h}) for

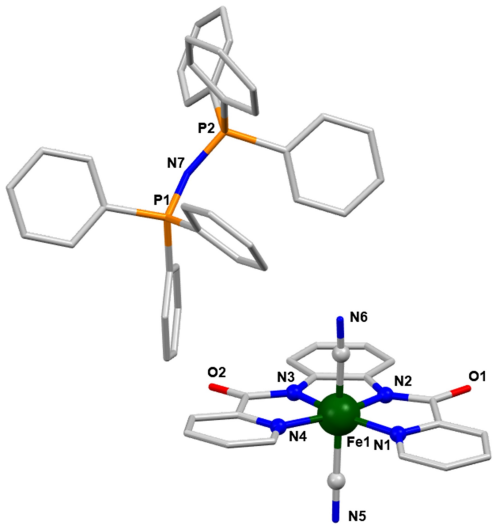

Figure 1. Molecular structure of $PNP[Fe^{III}(bpb)(CN)_2]$, **1 b**. Crystallization solvents and H atoms are not depicted for clarity.

Research Article
doi.org/10.1002/ejic.202400449

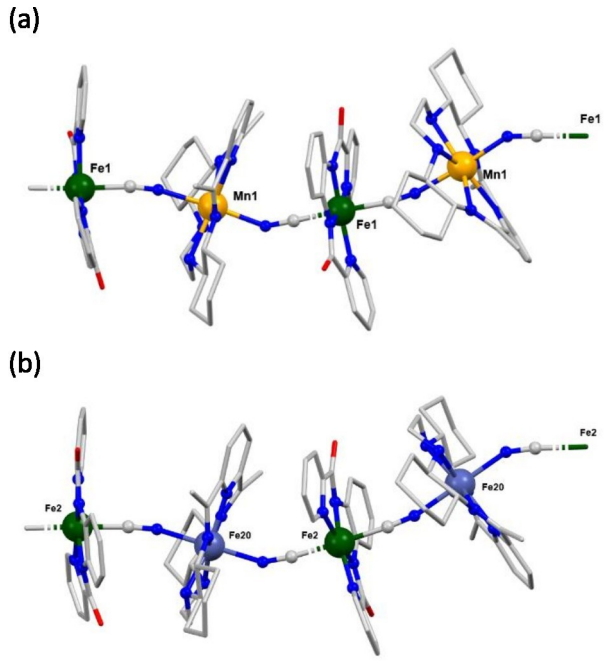

Figure 2. Molecular structure of (a) 1D-[{Fe^{III}(bpb)$(CN)_2$}{Mn^{II}-(L^R)}](PF_6)·MeOH·H_2O, **2R**, and (b) [{Fe^{III}(bpb)$(CN)_2$}{Fe^{II}-(L^R)}]$(ClO_4)_{0.4}Cl_{0.6}$·0.25MeOH 1.6H_2O, **4R**. The H-atoms, anions, and crystallization solvents are not depicted for clarity.

the two distinct Mn^{II} centers confirmed the distorted pentagonal bipyramid coordination sphere, with distortion comparable with those reported for related complexes.[30] The equatorial arrangement is responsible for this distortion (CShM parameters: 0.396–0.467 *versus* pentagonal), while axial alignment hardly deviates from linearity (Tables S2–S4). Mn–N equatorial distances (from 2.24 to 2.36 Å) and Mn–N axial distances (from 2.22 to 2.26 Å) substantiate the distortion of the PBP centers. One of the two Mn–N–C angles is significantly deviating from linearity with 144.5(3)°/145.8(3)° *versus* 167.5(3)°/164.0(3)° for the second. The CShM analysis for the Fe^{III} coordination sphere showed that coordination to Mn^{II} does not increase the distortion but deviation from O_h geometry remains important (Tables S5–S7). The Fe–C axial distances (1.95–1.97 Å), the Fe–N equatorial distances for amide moieties (1.88–1.98 Å), and the Fe–N equatorial distances for pyridine moieties (1.89–1.98 Å) confirm the equatorial distortion for the Fe complexes. The chains run in parallel along the *b*-direction (Figure SI14). A pseudo π-π stacking is observed along the *a*-direction that involves pyridyl moieties of neighboring chains, the distances between the ring centroids are 3.573 Å and 3.629 Å. The PF_6^- and the solvents molecules are located between these layers, some having H-bonds with the NH of the macrocycle (O103—H602, 2.190 Å) and the carbonyl of the bpb ligand (O1···O105, O51···O101; Figure S14). No direct H-bond interactions take place between chains. The shortest intermetallic distances are 5.0423(9) Å (Fe1···$Mn1_{1-x,\ -0.5+y,\ 1.5-z}$) and 5.1004(9) Å (Fe2···$Mn2_{1-x,\ -0.5+y,\ 1.5-z}$).

Powder X-ray diffraction for bulk samples of **2R**, **2S**, **3R**, and **3S** indicated that all derivatives have the same structural phase as described above for **2R** (Figure S11) with, however, the other enantiomer for the macrocyclic ligand when L^S is involved.

[{Fe^{III}(bpb)$(CN)_2$}{Fe^{II}(L^R)}]$(ClO_4)_{0.4}Cl_{0.6}$·0.25MeOH 1.6H_2O, **4R**, revealed a structure reminiscent to **2R** but with Fe(II) PBP units and different counter-anions (Figure 2b). The compound crystallized also in the chiral space group $P2_12_12_1$, and the asymmetric unit comprises the [Fe^{II}–Fe^{III}] moieties of two crystallographic independent 1D coordination polymers (Figure S15). These are made-up by the alternation of {Fe^{III}(bpb)$(CN)_2$} and {$Fe^{II}L^R$} units linked by the means of the cyanido-ligands. The heptacoordinated Fe^{II} units display homochiral L^R ligands and a coordination sphere corresponding to a slightly distorted PBP geometries (Table S2). The Fe–N bond lengths span from 2.152(4) to 2.309(7) Å (Figure S15). For the hexacoordinated [Fe^{III}-(bpb)$(CN)_2]^-$ centers, the distortion with respect to octahedral geometry is similar to that in **1b** and **2R**. Likewise, the bond lengths are in the range found in **2R**. The linkage of the cyanido-ligands to the Fe^{II} is slightly bent, with angles of about 153° and 167°. Overall, the geometric features and the molecular arrangement of the 1D coordination polymers in **4R** are very similar to that in **2R** (Figure S15). The closest contacts between chains are resulting from π-π-type interactions. The inter-chains distances between the Fe^{II} and Fe^{III} are 5.056(1) and 5.090(1) Å.

Circular Dichroism. The optical activity of **2R**, **2S**, **3R**, and **3S** was confirmed by the circular dichroism (CD) spectra recorded for crystalline sample diluted in KBr (0.25% in mass for **2R/S** and 1% for **3R/S**); the UV-vis spectra are given in Figure S19. The enantiomorphism of **2R** and **2S**, and **3R** and **3S** was confirmed by symmetrical spectra but with opposite sign (Figure 3). The CD features can be assigned to d-d and Ligand-to-Metal charge-transfer transitions[40] (400–800 nm) and intra-ligand π-π* transitions (200–350 nm). For **3R/S**, a strong component, centered at around 650 nm, is observed, which is not found for **2R/S**. This is due to the d-d transitions occurring in high-spin d^6 Fe^{II}, which are forbidden in the high-spin d^5 configuration of Mn^{II}. This specific CD band is found in the starting material [FeL(MeOH)Cl]Cl.[30]

Mössbauer spectroscopy. The ^{57}Fe Mössbauer spectroscopy was used to confirm the oxidation state of the Fe centers in the [Fe^{II}–Fe^{III}] chain compound. The spectrum recorded for polycrystalline **3R** at 80 K (Figure 4) consists of two doublets with chemical shift $\delta = 0.99(1)$ and 0.23(1) mm s^{-1}, and quadrupole splitting $\Delta E_Q = 3.18$ (2) and 1.10 (2) mm s^{-1}, respectively. The first doublet is characteristic for high-spin Fe^{II} ions in PBP geometry with N-bound cyanide-ligands in the apical positions.[18,21,41,42] The second is characteristic of octahedral Fe^{III} and its Mössbauer parameters closely resembles those of [Fe^{III}(bpb)$(CN)_2]^-$ and related low-spin derivatives.[35,40] It may be noticed that this isomer shift is slightly more positive in **3R** compared to the discrete complex (0.23 *versus* 0.085 mm s^{-1}) but remain clearly below the range found for the related high-spin Fe^{III} derivatives (i.e. about 0.5 mm s^{-1}).[35]

Magnetic properties. A solid-state EPR absorption spectrum was recorded for **1b** at 110 K (Figure 5). Analysis of the pattern gave best fit for $g_x = 2.22$, $g_y = 2.22$, and $g_z = 1.95$ with linewidth $\Delta H_x = \Delta H_y = 74.8$ Oe, and $\Delta H_z = 63$ Oe. The *g* values are compa-

Research Article
doi.org/10.1002/ejic.202400449

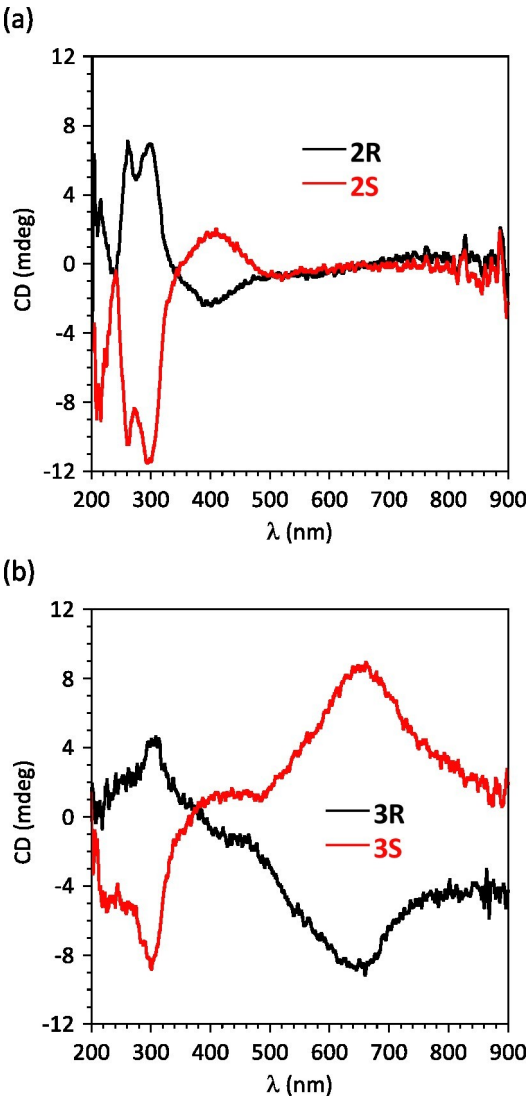

Figure 3. Solid-state CD spectra for (a) **2R** and **2S**, and (b) **3R** and **3S**.

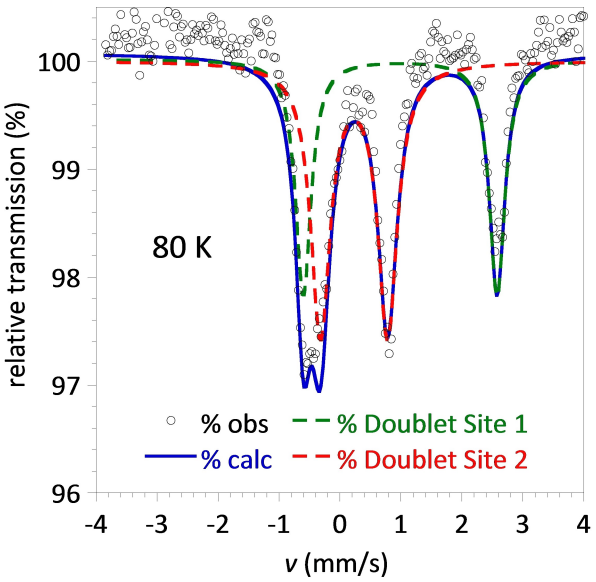

Figure 4. Mössbauer spectrum for **3R** at 80 K, site 1 and site 2 correspond to the Fe^{II} and the Fe^{III} centers respectively.

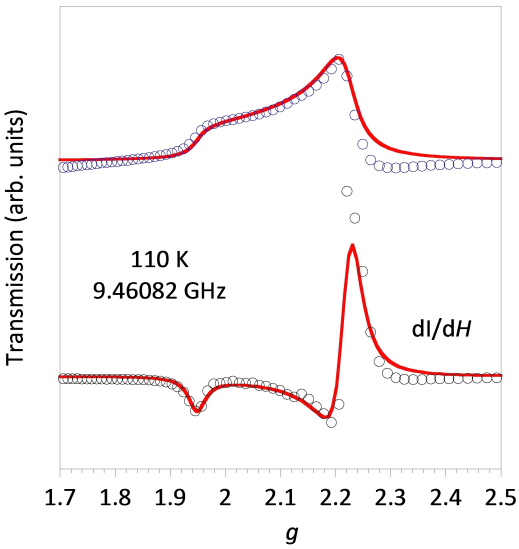

Figure 5. Solid state EPR for PNP[Fe^{III}(bpb)$(CN)_2$], **1 b**: Experimental (O) and calculated (—) spectrum at 110 K. Best-fit parameters are given in the main text.

rable to those reported for $NBu_4[Fe^{III}(bpb)(CN)_2]$ in solution.[35] The anisotropy of ΔH reveals anisotropy in spin-phonon coupling.[43]

The solid state magnetic behaviors were investigated for **1 b**, and for one enantiomer of the chain compounds, **2R** and **3S**, since chirality does not affect the magnetic properties. For **1 b**, the temperature dependence of the molar magnetic susceptibility, χ_M, shows a slight decrease of $\chi_M T$ from 0.45 $cm^3 mol^{-1} K$ at 300 K to 0.39 $cm^3 mol^{-1} K$ for 2 K (Figure S16). This behavior is consistent with previous reports[35,39,40] and confirms a $S=\frac{1}{2}$ ground spin state slightly deviating from Curie behavior. The field dependence of the magnetization for different temperature between 2 and 4 K are in agreement with this spin state (Figure S16). The magnetic behavior have been modeled for an $S=\frac{1}{2}$ spin with a temperature independent contribution (TIP) using PHI.[44] Best fit to $\chi_M T$ versus T and M versus H gave $g=2.04$ and TIP $=(198.3\pm0.4)\times10^{-6}$ $cm^3 mol^{-1}$.

For **2R**, the variation of $\chi_M T$ versus T (Figure 6) is characterized by a continuous decrease from 4.85 $cm^3 mol^{-1} K$ at 300 K to 2.87 $cm^3 mol^{-1} K$ for 2 K. The value at high temperature is in agreement with the anticipated 4.8 $cm^3 mol^{-1} K$ contributed by one $S=5/2$ and one $S=\frac{1}{2}$ [Fe^{III}(bpb)$(CN)_2$] center in the absence of exchange interactions. The observed $\chi_M T$ versus T behavior suggests that antiferromagnetic interactions take place between the Mn^{II} and the Fe^{III} centers but the spin-chain regime is not reached at 2 K. This is supported by the M versus H at 2 K that shows a rather gradual and continuous increase of M with field to reach 5.05 μ_B for 70 kOe but saturation is not observed. A Curie-Weiss analysis ($\chi_M = C/(T-\theta)$, Figure S17) gave $C=4.8$ $cm^3 mol^{-1} K$ and $\theta=-5.0$ K, thus confirming the antiferromagnetic Mn^{II}–Fe^{III} interactions. An evaluation of the exchange interaction was obtained by modeling the $\chi_M T$ versus

Research Article
doi.org/10.1002/ejic.202400449

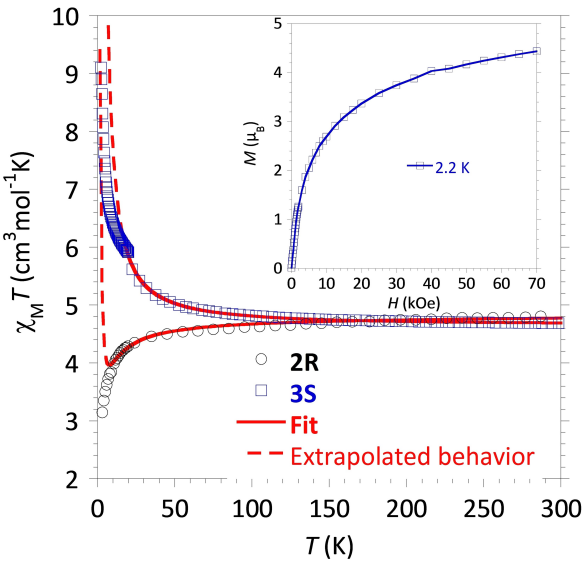

Figure 6. Temperature dependence of $\chi_M T$ for **2R** and **3S** with modeling (—), and (insert) field dependence of the magnetization of **3S** at 2.2 K. The dashed lines are the calculated behaviors extrapolated to 2 K.

T behavior using an expression of the susceptibility for Heisenberg linear chains with alternating spins.[45,46] A TIP contribution arising for the Fe^{III} units was included to account for the steady increase of $\chi_M T$ with T in the higher T domain. Best fit to the experimental behavior between 10 and 300 K gave $J_{MnFe} = -1.98 \pm 0.01$ cm^{-1} with $g_{Mn} = 2.0$ (fixed), $g_{Fe} = 2.1$ (fixed) and TIP $= (105 \pm 10) \times 10^{-6}$ cm^3 mol^{-1}. The strength of the Fe–Mn interaction obtained for **2R** is similar to values reported for related chain compounds.[31] The antiferromagnetic exchange interaction is in agreement with the overlap scheme of the magnetic orbitals of each metal ion mediated by the cyanide-ligand.[47] The t_{2g} orbitals of Fe^{III}, which carry the unpaired electron, overlap with the singly occupied π-type orbitals of Mn^{II} (i.e. d_{xy}, d_{xz}, and d_{yz}) via the π-orbitals of the bridging ligand, but are orthogonal to the magnetic σ-type orbitals (d_{z^2} and $d_{x^2-y^2}$) of this ion. The result is three antiferromagnetic and two ferromagnetic exchange pathways, leading to a weak overall antiferromagnetic behavior.

For a ferrimagnetic chain, a divergence of $\chi_M T$ is expected as T is lowered, and even for a weak interaction, such as in **2R**, an increase in $\chi_M T$ should be observed above 2 K (see Figure 6). The lack of $\chi_M T$ rise for **2R** suggests that inter-chain antiferromagnetic interactions come into play at low temperatures. Such inter-chain magnetic interactions can be favored by the π-π stacking, involving pyridyl groups bonded to the metal centers, between adjacent 1D architectures (Figure S14).

The temperature dependence of $\chi_M T$ for **3S** shows a continuous increase as T is lowered (Figure 6), a characteristic for ferromagnetic interactions between the metal ions. At 300 K, $\chi_M T$ has a value of 4.68 cm^3 mol^{-1} K, slightly above the 4.0 cm^3 mol^{-1} K expected for one Fe^{II} ($S = 2$, $g = 2.20$) in PBP environment[41] and the Fe^{III} unit in the absence of exchange interactions. For 2 K, $\chi_M T$ reaches 9.10 cm^3 mol^{-1} K. The M versus H at 2.2 K (Figure 6, insert) shows a fast increase of M for small fields, a behavior consistent with a growth of the exchange correlation along the chain. For fields above 10 kOe, the increase of M is more gradual to reach 4.4 μ_B for 70 kOe without saturation. The magnetization plots at 5 and 8 K (Figure S18) show a more gradual raise of M for weak fields, suggesting the loss of the exchange correlation for these temperatures. The Curie-Weiss analysis (Figure S18) gave $C = 4.6$ cm^3 mol^{-1} K and $\theta = 4.0$ K. The positive value for θ supports ferromagnetic Fe^{II}–Fe^{III} interactions. This is again rationalized by the magnetic orbital interactions. For high-spin Fe^{II} in PBP geometry, the singly occupied orbitals comprise two sigma- and two π-type orbitals,[17] leading respectively to ferro- and antiferro-magnetic exchange pathways with the Fe^{III} unit. However, one of the latter must be very weak because of the poor overlap between the d_{xy} orbital of Fe^{II} with the π-system of the cyanide ligand linked in the apical positions, therefore the overall Fe^{II}–Fe^{III} exchange interaction is ferromagnetic. A related ferromagnetic interaction was observed between PBP Fe^{II} and a Cr^{III} cyanometallate,[42] which involves the same magnetic orbitals as the Fe^{III} unit.

The $\chi_M T$ versus T behavior was analyzed using the model for 1D spin arrays discussed above, best fit to the experimental data between 15 and 300 K (Figure 6) gave $J_{FeFe} = 3.49 \pm 0.01$ cm^{-1}, $g_{Fe^{II}} = 2.36$, $g_{Fe^{III}} = 2.10$ (fixed), TIP $= (8 \pm 2) \times 10^{-5}$ cm^3 mol^{-1}.

The occurrence of slow relaxation of the magnetization in **3S**, possibly induced by the easy-axis magnetic anisotropy (i.e. $D < 0$) exhibited by the PBP Fe^{II} centers,[17,30] was assessed by AC susceptibility (Figure S18). Only the onset of an out-of-phase component of the magnetic susceptibility, χ_M'', was observed below 3 K for a test frequency of 1 kHz in the absence of a static applied magnetic field. The application of a field led to a decrease of both χ_M' and χ_M'' signals. No further investigation was performed but the appearance of a χ_M'' component suggests that **3S** may behave as a SCM below 2 K. This emergence of slow magnetization relaxation only at very low temperatures can be paralleled by the weak exchange interactions taking place in this compound.

3. Concluding Remarks

The results gathered validate the suitability of the chiral PBP complexes [MnL(MeOH)Cl]Cl[36] or [FeL(MeOH)Cl]Cl[30] (with L either L^R or L^S) to be used as building block to achieve chiral spin chains by association with a trans-dicyanido metallo-ligand. Optical dichroism confirmed the enantiomorphism of the compounds obtained with the L^R and L^S macrocyclic ligands.

The magnetic behavior for the spin chains shows that the exchange interactions taking place between Mn^{II} or Fe^{II} and the metallo-ligand $[Fe^{III}(bpb)(CN)_2]^-$ are weak. Nevertheless, the onset of SCM behavior is suggested by the AC susceptibility obtained for the [Fe^{II}–Fe^{III}] chain **3S**, but improvement of this behavior will require stronger exchange interactions. In this respect, another metallo-ligand with larger spin state or involving a 4 d or 5 d metal ion could be considered.

Research Article
doi.org/10.1002/ejic.202400449

Experimental

Reagents and solvents were used as received from commercial sources unless otherwise specified. All operations involving Fe(II) were carried out in a glovebox under an Ar atmosphere, and reagents and solvents were deoxygenated. [MnL(MeOH)Cl]Cl,[36] [FeL(MeOH)Cl]Cl,[30] and $NBu_4[Fe^{III}(bpb)(CN)_2]$, **1 a**,[35] complexes were synthesized following published procedures. For the latter compound some adaptations have been made, a detailed description is given in the SI.

Preparation of 1D-[{Fe^{III}(bpb)$(CN)_2$}{$M^{II}(L^{R/S})$}](PF_6) Derivatives 2R, 2S, 3R, and 3S

1D-[{Fe^{III}(bpb)$(CN)_2$}{$Mn^{II}(L^R)$}](PF_6)·MeOH·H_2O, 2R: Compound **1 a** (223 mg, 0.335 mmol) was dissolved in methanol (20 mL). [Mn^{II}-(L^R)(Cl)(MeOH)](Cl) (0.335 mmol) was dissolved in a mixture of methanol (15 mL) and dichloromethane (5 mL), NH_4PF_6 (55 mg, 0.335 mmol) was added and the solution stirred for a few minutes. The two solutions were layered in a test tube with a MeOH layer (5 mL) in between. Crystals of **2R** suitable for X-Ray diffraction were obtained after few days by slow liquid-liquid inter-diffusion of the two reactant solutions. The crystals were washed with a minimum of methanol and dried by nitrogen flux, yielding 138 mg (Y = 39 %) of **2R**.

The same procedure was applied for the syntheses of **2S**, **3R**, and **3S**, but using the adapted PBP complex.

2R: IR (ATR germanium, cm^{-1}) 2919 (w), 2850 (w), 2127 (w), 1614 (m), 1589 (s), 1575 (m), 1471 (m), 1451 (w), 1361 (m), 1297 (w), 1253 (w), 1194 (w), 1140 (w), 1109 (w), 1031 (w), 959 (w), 908 (w), 841 (vs), 812 (m), 797 (m), 691 (w), 644 (w), 627 (w), 606 (w). Elemental analysis (%) calcd. $C_{44}H_{53}F_6FeMnN_{11}O_4P$ (**2R**, 1D-[{Fe^{III}(bpb)$(CN)_2$}{$Mn^{II}(L^R)$}](PF_6)·MeOH·H_2O): C 50.06; H 5.06; N 14.59; found: C 50.14; H 4.77; N 14.71.

2S: Y = 21 %. IR (ATR germanium, cm^{-1}) 2931 (w), 2863 (w), 2126 (w), 1612 (m), 1589 (s), 1587 (m), 1561 (m), 1470 (w), 1445 (m), 1355 (m), 1295 (w), 1251 (w), 1240 (w), 1192 (w), 1158 (w), 1140 (w), 1125 (w), 1107 (w), 1096 (w), 1082 (w), 1058 (w), 1045 (w), 1034 (w), 1019 (w), 991 (w), 958 (w), 928 (w), 906 (w), 875 (w), 836 (vs), 810 (m), 788 (m), 766 (m), 759 (m), 745 (m), 739 (w), 727 (w), 700 (w), 690 (w), 674 (w), 650 (w), 615 (w), 608 (w). Elemental analysis (%) calcd. $C_{44}H_{53}F_6FeMnN_{11}O_4P$ (**2S**, 1D-[{Fe^{III}(bpb)$(CN)_2$}{Mn^{II}-(L^R)}](PF_6)·MeOH·H_2O): C 50.06; H 5.06; N 14.59; found: C 49.96; H 5.13; N 14.56.

3R: Y = 55 %. IR (ATR germanium, cm^{-1}) 2938 (w), 2867 (w), 2128 (w), 1614 (m), 1589 (s), 1575 (m), 1563 (m), 1471 (m), 1449 (m), 1360 (m), 1296 (w), 1259 (w), 1141 (m), 1122 (w), 1096 (w), 1045 (w), 1034 (w), 959 (w), 841 (vs), 809 (m), 766 (m), 691 (m). Elemental analysis (%) calcd. $C_{44}H_{53}F_6FeMnN_{11}O_4P$ (**3R**, 1D-[{Fe^{III}(bpb)$(CN)_2$}{Fe^{II}-(L^R)}](PF_6)·H_2O): C 50.41; H 4.82; N 15.04; found: C 50.45; H 5.02; N 14.70.

3S: Y = 62 %. IR (ATR germanium, cm^{-1}) 2963 (w), 2938 (w), 2865 (w), 2125 (w), 1616 (m), 1590 (s), 1573 (m), 1470 (m), 1451 (m), 1358 (m), 1296 (w), 1262 (m), 1140 (m), 1097 (m), 1034 (m), 959 (w), 841 (vs), 808 (s), 763 (m), 690 (w), 652 (w), 642 (w), 608 (w). Elemental analysis (%) calcd. $C_{44}H_{53}F_6FeMnN_{11}O_4P$ (**3S**, 1D-[{Fe^{III}(bpb)$(CN)_2$}{$Fe^{II}(L^S)$}](PF_6)·H_2O): C 50.41; H 4.82; N 15.04; found: C 50.55; H 4.79; N 14.68.

1D-[{Fe^{III}(bpb)$(CN)_2$}{$Fe^{II}(L^R)$}]$(ClO_4)_{0.4}Cl_{0.6}$·0.25MeOH·1.6H_2O, 4R: Compound **1 a** (12 mg, 0.018 mmol) was dissolved in methanol (1.3 mL). [$Fe^{II}(L^R)$(Cl)(MeOH)](Cl) (10 mg, 0.0215 mmol) and $NaClO_4$ (2 mg; 0.09 mmol) were dissolved in a mixture of methanol (1.4 mL) and dichloromethane (0.7 mL). The two solutions were layered in a test tube with a MeOH layer (2 mL) in between. Crystals of **4R** suitable for X-Ray diffraction were obtained after few days by slow liquid-liquid inter-diffusion of the two reactant solutions. The crystals were washed with a minimum of methanol and dried with diethyl ether, yielding 7.8 mg (Y = 40 %) of **4R**.

IR (ATR germanium, cm^{-1}) 2938 (w), 2865 (w), 2128 (w), 1613 (m), 1588 (s), 1575 (m), 1562 (m), 1470 (m), 1448 (m), 1360 (m), 1296 (w), 1259 (w), 1140 (m), 1091 (vs), 1033 (w), 959 (w), 929 (w), 887 (w), 810 (m), 768 (m), 691 (m), 623 (m).

Acknowledgements

DM thanks the University of Toulouse for the award of a thesis grant. Authors are grateful to Mrs. G. Ballon and Dr L.-M. Lacroix (INSA Toulouse) for magnetic data collection, to Dr. L. Vendier and J.-F. Meunier for recording capillary powder X-ray and Mössbauer data, and to Mrs C. Barthes (LCC) for assistance for the syntheses of the ligands.

Conflict of Interests

The authors declare no conflict of interest.

Data Availability Statement

The data that support the findings of this studies are available from the corresponding author upon reasonable request.

Keywords: Chain structures · Chirality · Heterometallic complex · Magnetic properties · Pentagonal bipyramidal compound · Macrocyclic ligand

[1] M. Verdaguer, G. S. Girolami, *Magnetism: Molecules to materials*, Vol. 5 (Eds: J. S. Miller, M. Drillon), Wiley-VCH, Weinheim **2005**, pp. 283–346.
[2] K. S. Pedersen, J. Bendix, R. Clerac, *Chem. Commun.* **2014**, *50*, 4396–4415.
[3] M. Zhu, L. Li, J.-P. Sutter, *Inorg. Chem. Front.* **2016**, *3*, 994–1003.
[4] J. Ferrando-Soria, J. Vallejo, M. Castellano, J. Martínez-Lillo, E. Pardo, J. Cano, I. Castro, F. Lloret, R. Ruiz-García, M. Julve, *Coord. Chem. Rev.* **2017**, *339*, 17–103.
[5] E. Coronado, *Nat. Rev. Mater.* **2020**, *5*, 87–104.
[6] D. Shao, X.-Y. Wang, *Chin. J. Chem.* **2020**, *38*, 1005–1018.
[7] A. E. Thorarinsdottir, T. D. Harris, *Chem. Rev.* **2020**, *120*, 8716–8789.
[8] M. R. Wasielewski, M. D. E. Forbes, N. L. Frank, K. Kowalski, G. D. Scholes, J. Yuen-Zhou, M. A. Baldo, D. E. Freedman, R. H. Goldsmith, T. Goodson, M. L. Kirk, J. K. McCusker, J. P. Ogilvie, D. A. Shultz, S. Stoll, K. B. Whaley, *Nat. Rev. Chem.* **2020**, *4*, 490–504.
[9] R. A. Murphy, J. R. Long, T. David Harris, *Commun. Chem.* **2021**, *4*, 70.
[10] J.-H. Wang, Z.-Y. Li, M. Yamashita, X.-H. Bu, *Coord. Chem. Rev.* **2021**, *428*, 213617.
[11] S. Barman, A. Pal, A. Mukherjee, S. Paul, A. Datta, S. Ghosh, *Chem. Eur. J.* **2024**, *30*, e202303120.
[12] S.-Q. Su, S.-Q. Wu, S. Kanegawa, K. Yamamoto, O. Sato, *Chem. Sci.* **2023**, *14*, 10631–10643.
[13] J. Long, *Front. Chem.* **2019**, *7*, 63.
[14] K. S. Pedersen, P. Perlepe, M. L. Aubrey, D. N. Woodruff, S. E. Reyes-Lillo, A. Reinholdt, L. Voigt, Z. Li, K. Borup, M. Rouzières, D. Samohvalov, F. Wilhelm, A. Rogalev, J. B. Neaton, J. R. Long, R. Clérac, *Nat. Chem.* **2018**, *10*, 1056–1061.

[15] C. Coulon, H. Miyasaka, R. Clérac, in *Single-Molecule Magnets and Related Phenomena*, Vol. 122 (Ed: R. Winpenny), Springer, Berlin **2006**, pp. 163–206.
[16] C. Coulon, V. Pianet, M. Urdampilleta, R. Clérac, in *Molecular Nanomagnets and Related Phenomena*, Vol. 164 (Ed: S. Gao), Springer Berlin, Heidelberg **2015**, pp. 143–184.
[17] J.-P. Sutter, V. Béreau, V. Jubault, K. Bretosh, C. Pichon, C. Duhayon, *Chem. Soc. Rev.* **2022**, *51*, 3280–3313.
[18] T. S. Venkatakrishnan, S. Sahoo, N. Bréfuel, C. Duhayon, C. Paulsen, A.-L. Barra, S. Ramasesha, J.-P. Sutter, *J. Am. Chem. Soc.* **2010**, *132*, 6047–6056.
[19] D. Shao, X.-H. Zhao, S.-L. Zhang, D.-Q. Wu, X.-Q. Wei, X.-Y. Wang, *Inorg. Chem. Front.* **2015**, *2*, 846–853.
[20] B. Drahoš, R. Herchel, Z. Trávníček, *Inorg. Chem.* **2018**, *57*, 12718–12726.
[21] C. Pichon, N. Suaud, C. Duhayon, N. Guihéry, J.-P. Sutter, *J. Am. Chem. Soc.* **2018**, *140*, 7698–7704.
[22] K. Bretosh, V. Béreau, C. Duhayon, C. Pichon, J.-P. Sutter, *Inorg. Chem. Front.* **2020**, *7*, 1503–1511.
[23] X.-D. Zheng, L. Jiang, X.-L. Feng, T.-B. Lu, *Dalton Trans* **2009**, 6802–6808.
[24] E. Pardo, C. Train, R. Lescouezec, Y. Journaux, J. Pasan, C. Ruiz-Perez, F. S. Delgado, R. Ruiz-Garcia, F. Lloret, C. Paulsen, *Chem. Commun.* **2010**, *46*, 2322–2324.
[25] J. Ru, F. Gao, T. Wu, M.-X. Yao, Y.-Z. Li, J.-L. Zuo, *Dalton Trans.* **2014**, *43*, 933.
[26] C. Pichon, C. Duhayon, E. Delahaye, J.-P. Sutter, *Eur. J. Inorg. Chem.* **2021**, *2021*, 5112–5118.
[27] A. Choudhury, C. Pichon, J.-P. Sutter, D. Pamu, B. Sarma, P. P. Mudoi, N. Gogoi, *Chem. Commun.* **2021**, *57*, 207–210.
[28] K. Dhbaibi, M. Grasser, H. Douib, V. Dorcet, O. Cador, N. Vanthuyne, F. Riobé, O. Maury, S. Guy, A. Bensalah-Ledoux, B. Baguenard, G. L. J. A. Rikken, C. Train, B. Le Guennic, M. Atzori, F. Pointillart, J. Crassous, *Angew. Chem. Int. Ed.* **2023**, *62*, e202215558.
[29] T. Ekanayaka, T. Jiang, E. Delahaye, O. Perez, J.-P. Sutter, D. Le, A. T. N'Diaye, R. Streubel, T. S. Rahman, P. A. Dowben, *Phys. Chem. Chem. Phys.* **2023**, *25*, 6416–6423.
[30] V. Jubault, B. Pradines, C. Pichon, N. Suaud, C. Duhayon, N. Guihéry, J.-P. Sutter, *Cryst. Growth Des.* **2023**, *23*, 1229–1237.
[31] D. Zhang, H. Wang, Y. Chen, Z.-H. Ni, L. Tian, J. Jiang, *Inorg. Chem.* **2009**, *48*, 5488–5496.
[32] Z.-H. Ni, H.-Z. Kou, Y.-H. Zhao, L. Zheng, R.-J. Wang, A.-L. Cui, O. Sato, *Inorg. Chem.* **2005**, *44*, 2050–2059.
[33] D. Zhang, L. Kong, H. Zhang, K. Chen, *J. Coord. Chem.* **2015**, *68*, 3969–3981.
[34] D. Zhang, H. Zhang, *Polyhedron* **2015**, *100*, 36–42.
[35] S. K. Dutta, U. Beckmann, E. Bill, T. Weyhermüller, K. Wieghardt, *Inorg. Chem.* **2000**, *39*, 3355–3364.
[36] K. Aston, N. Rath, A. Naik, U. Slomczynska, O. F. Schall, D. P. Riley, *Inorg. Chem.* **2001**, *40*, 1779–1789.
[37] S. Alvarez, P. Alemany, D. Casanova, J. Cirera, M. Llunell, D. Avnir, *Coord. Chem. Rev.* **2005**, *249*, 1693–1708.
[38] M. Llunell, D. Casanova, J. Cirera, P. Alemany, S. Alvarez, SHAPE: Program for the stereochemical analysis of molecular fragments by means of continuous shape measures and associated tools 2.1 ed., University of Barcelona, Barcelona **2013**.
[39] X. Chen, L. Kong, H. Zhang, D. Zhang, *Asian J. Chem.* **2015**, *27*, 3373–3376.
[40] M. Ray, R. Mukherjee, J. F. Richardson, R. M. Buchanan, *J. Chem. Soc., Dalton Trans.* **1993**, 2451–2457.
[41] A. K. Bar, N. Gogoi, C. Pichon, V. M. L. D. P. Goli, M. Thlijeni, C. Duhayon, N. Suaud, N. Guihéry, A.-L. Barra, S. Ramasesha, J.-P. Sutter, *Chem. Eur. J.* **2017**, *23*, 4380–4396.
[42] C. Pichon, N. Suaud, V. Jubault, C. Duhayon, N. Guihéry, J.-P. Sutter, *Chem. Eur. J.* **2021**, *27*, 15484–15495.
[43] H. Yamaguchi, Y. Tominaga, A. Matsuo, S. Morota, Y. Hosokoshi, M. Hagiwara, K. Kindo, *Phys. Rev. B* **2023**, *107*, 174422.
[44] N. F. Chilton, R. P. Anderson, L. D. Turner, A. Soncini, K. S. Murray, *J. Comput. Chem.* **2013**, *34*, 1164–1175.
[45] M. Drillon, E. Coronado, D. Beltran, R. Georges, *Chem. Phys.* **1983**, *79*, 449–453.
[46] R. Georges, J. J. Borras-Almenar, E. Coronado, J. Curély, M. Drillon, in *Magnetism: Molecules to materials: Models and experiments*, Vol. 1 (Eds: M. Miller, J. S. Drillon), Wiley-VCH, Weinheim **2002**, pp. 1–47.
[47] M. Verdaguer, A. Bleuzen, V. Marvaud, J. Vaissermann, M. Seuleiman, C. Desplanches, A. Scuiller, C. Train, R. Garde, G. Gelly, C. Lomenech, I. Rosenman, P. Veillet, C. Cartier, F. Villain, *Coord. Chem. Reviews* **1999**, *190–192*, 1023–1047.

Manuscript received: July 17, 2024
Revised manuscript received: September 9, 2024
Accepted manuscript online: September 23, 2024
Version of record online: ■■, ■■

RESEARCH ARTICLE

Chiral 1D coordination compounds, formed by association of either of the enantiomers of pentagonal bipyramidal Fe^{II} and Mn^{II} complexes based on an homochiral macrocyclic ligand, and a *trans*-dicyanido Fe^{III} metalloligand are reported. Their preparations, crystal structures, optical and magnetic properties are discussed.

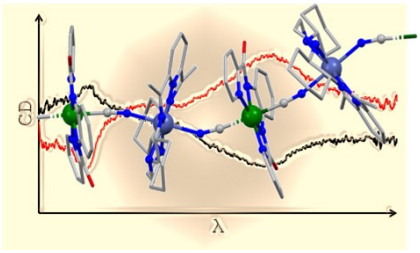

*D. Martinez, C. Pichon, C. Duhayon, V. Béreau, H. Yamaguchi, J.-P. Sutter**